Journal of the Korean Chemical Society
2013, *Vol. 57, No. 1*
Printed in the Republic of Korea
http://dx.doi.org/10.5012/jkcs.2013.57.1.109

Effects of Aluminum Nanoparticles on Thermal Decomposition of Ammonium Perchlorate

Yan-Li Zhu*, Hao Huang†, Hui Ren, and Qing-Jie Jiao

*State Key Laboratory of Explosive Science and Technology, Beijing Institute of Technology, South Street No. 5, Zhongguancun, Haidian District, Beijing, 100081, China. *E-mail: zhuyanli1999@bit.edu.cn*
†China North Chemical Industries Group CO. LTD, 11F North Real Estate Building No.81 Zizhuyuan Road, Haidian District,100089, China
(Received June 14, 2012; Accepted December 31, 2012)

ABSTRACT. The effects of aluminum nanoparticles (AlNs) on the thermal decomposition of ammonia perchlorate (AP) were investigated by DSC, TG-DSC and DSC-TG-MS-FTIR. Addition of AlNs resulted in an increase in the temperature of the first exothermic peak of AP and a decrease in the second. The processing of non-isothermal data at various heating rates with and without AlNs was performed using Netzsch Thermokinetics. The dependence of the activation energy calculated by Friedman's isoconversional method on the conversion degree indicated the decomposition process can be divided into three steps. They were C1/D1/D1 for neat AP, determined by Multivariate Non-linear Regression, and changed to C1/D1/F2 after addition of AlNs into AP. The isothermal curves showed that the thermal stability of AP in the low temperature stage was improved in the presence of AlNs.

Key words: Aluminum nanoparticle, Thermal decomposition, Ammonium perchlorate, Explosive

INTRODUCTION

Ammonium perchlorate (AP) is an oxidizing component, which has been excellently applied in various propellants and pyrotechnics.[1] The thermal decomposition characteristics of AP play a key role in the combustion behavior of composite solid propellants and are sensitive to the presence of additives, which are used to improve the performance of the propellants.[2] The most commonly used additives are metal oxides[2–10] and metal powders.[11–16] In recent years, new additives based on nanometer particles are being considered in this propulsion application, mainly due to their large specific surface area and high reactivity.[17]

Aluminum nanoparticles (AlNs) is of special interest and an important ingredient in contemporary composite solid propellants since Al is a metallic fuel in the propellant formulation which reacts and releases significant chemical energy and increases the specific impulse.[17–18] Simultaneously, it is a catalyst for the thermal decomposition of AP. The performance of propellants is highly relevant to the interaction between AP and AlNs. However, few studies have reported the effects of AlNs on the thermal decomposition of AP. Liu et al.[15,19] concluded that the thermal decomposition of neat AP was divided into two processes with the low-temperature decomposition (LTD) process and the high-temperature one (HTD). The first temperature was increased with the presence of AlNs and the second was decreased. While Zhi and his co-workers[14] reported addition of AlNs has almost no effect on the thermal decomposition of AP by Thermogravimetry (TG) and Differential Scanning Calorimetry (DSC). This difference indicates it is necessary to make a systematic study on the effects of AlNs additives on AP thermal decomposition and figure out the underlying catalytic mechanism of AlNs.

In the present study, the effects of AlNs on thermal decomposition of AP were examined with the aid of a set of specific experimental devices DSC-TG-MS-FTIR. The main purpose of this paper is to provide some experimental information on thermal-decomposition kinetics of AP in the presence of AlNs.

EXPERIMENTAL

Materials and Characterization

AP (Dalian Potassium Chlorate Works, China, >99%) was analytical grade. The average particle size of Al powders (Xuzhou Jiechuang New Material CO., LTD., China, 99.9%) was 40 nm. AP/Al mixtures were prepared by mixing the two components in a polished carnelian mortar for 1 hr.

Thermal Analysis

A Netzsch STA449C, Netzsch-QMS403C and Nicolet

6700 FTIR coupling system (DSC-TG-MS-FTIR) was used for thermal analysis. The ionizing electron energy of Netzsch-QMS403C is 70 eV. The pressure injection of the quartz capillary gas connector is 1 bar and the capillary temperature is 200 °C. The resolution of Nicolet 6700 FTIR is 4 cm^{-1}. The gas cell and gas tube between TG/DSC and FTIR stay at 200 °C.

A sample with the mass of ~2 mg placed in an aluminum crucible with a pre-hole on the lid was heated from 30 °C to 500 °C. α-Al_2O_3 was used as the reference sample. High-purity argon was used with a gas flow rate of 20 mL/min.

Four weight contents, 0%, 14%, 27% and 40%, of Al powders in AP formulations were analyzed by DSC with a rate of 10 K/min. Non-isothermal thermal decomposition of neat AP and AP/Al (60/40) mixture was performed at the rates of 5, 10, 15 and 20 K/min. The non-isothermal data were processed by "Netzsch Thermokinetics". The details of this program can be found elsewhere.[20] The model-free Friedman method was used to obtain the dependence of the activation energy on conversion degree. "Multivariate Non-linear Regression" was used to evaluate and decide the complex mechanism of the investigated process and corresponding kinetic parameters.

The thermal decomposition process of AP and AP/Al (60/40) mixture was monitored by MS and FTIR on-line with the heating rate of 10 K/min. The MS and FTIR results can provide some information about the produced gases and chemical reactions occurring during thermal decomposition.

RESULTS AND DISCUSSION

DSC Analysis

The DSC curves of the AP/40 nm Al mixture at the heat rate of 10 K/min with four Al content levels are given in *Fig*. 1. The thermogram for neat AP has an endothermic temperature of about 242 °C, which is ascribed to the transition from the orthorhombic to the cubic phase,[21] and two exotherms with peak maximum temperatures of 323 °C and 423 °C, respectively. The first or low-temperature exothermic peak was confirmed to the partial decomposition of AP and an intermediate product was formed simultaneously. The second or high-temperature exothermic peak corresponded to complete decomposition of the intermediate product into volatile products.[19]

The addition of nano-sized Al powders into AP has little effect on the endothermic peaks of all AP/Al mixtures, while the first exothermic peak of AP/Al (86/14) tended to

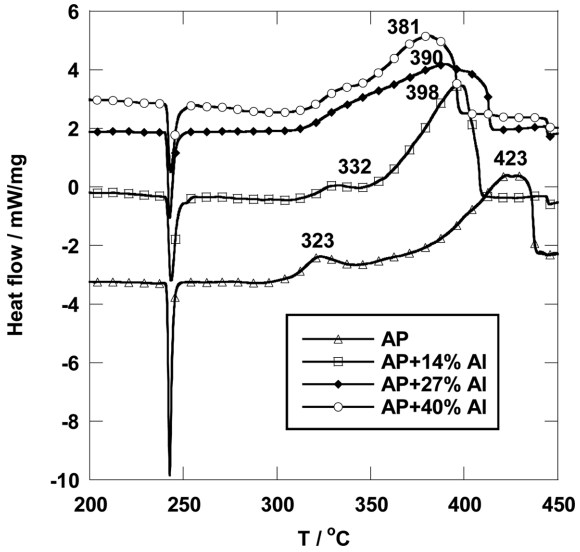

***Fig.* 1.** DSC curves of AP with 0, 14, 27, 40 wt% 40 nm Al at a heating rate of 10 K/min.

weaken and shifted to 332 °C compared to neat AP, and the second one became stronger and moved to the lower temperature side at 398 °C. The position in the first exothermic peak changed slowly with the increasing of Al content, while it was more pronounced for the second peak. These two exothermic peaks were combined into one at 381 °C when Al content was 40%, indicating that Al nanoparticles show an excellent catalytic effect on HTD of AP by lowering the temperature of 42 °C and an inhibition on LTD of AP. More noticeably, the heat release of AP was increased greatly in the presence of nano-sized Al. The heat releases of the AP/Al mixtures with the Al content of 14%, 27% and 40% were 1.07, 1.16 and 1.25 kJ per gram of AP, respectively, compared to 0.72 kJ/g for neat AP.

It is known that the thermal decomposition of AP starts with sublimation and dissociation:

$$NH_4ClO_4 \leftrightarrow NH_4^+ + ClO_4^- \quad (1)$$

LTD of AP[22] is considered to begin with the proton transfer from cation to anion likely to occur at the intersections of dislocations in the bulk crystals. It performs not at the very surface but in pores beneath it at a distance of about several microns. In the case of AP/Al mixture, AlNs were likely to be absorbed onto the surface of AP. Therefore, the sublimation and dissociation of AP were inhibited. In addition, AlNs may be also absorbed onto the sub-surface of AP and decrease the number of the dislocation. This is not favorable for Eq. (1) towards to the right. Thus, the first exothermic peak temperature of AP

increased in the presence of AlNs.

The changes in HTD of AP with the existence of AlNs may be caused by two reasons. One is related to the huge surface area of AlNs. AlNs can absorb many gaseous reactive molecules onto their surface, and catalyze their reactions. The other is that HTD of AP can be catalyzed indirectly by AlN, which is an active metal with a high reactivity, and can react easily with the decomposition products of AP.[23] However, the amount of Al involved in these reactions is probably small because most nano-sized Al is not oxidized until the temperature is above 500 °C.[24] Since most reactions between AlNs and the decomposition products of AP are exothermic, the heat release of AP was increased in the presence of AlNs.

Non-Isothermal Thermal Analysis

Fig. 2 shows the TG-DSC curves of AP/Al (60/40) mixture with the heat rates of 5, 15 and 20 K/min. The onset, peak and end temperatures of the thermal decomposition process of this mixture increased with the increasing of the heating rate, while the position of crystalloid transition temperature changed little. The similar trends (not shown here) were also obtained for neat AP.

The model-free Friedman method was applied to obtain the dependence of activation energy E on conversion degree α based on the data in *Fig*. 2. The results shown in *Fig*. 3 indicate that the thermal decomposition process is complex and can be divided into three steps. The first step is from 0 to 7%, where the activation energy is between 130–200 kJ/mol. The second is from 7% to 17%, where the activation energy is between 130–160 kJ/mol. The last is from 17% to the end with the activation energy of 120–160 kJ/mol. Therefore, a three-step model of A→B→C→D

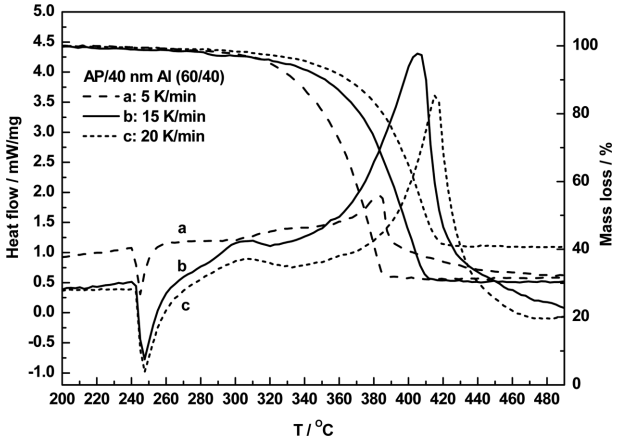

***Fig*. 2.** TG-DSC curves of AP/Al (60/40) mixture at heating rates of 5, 15, 20 K/min.

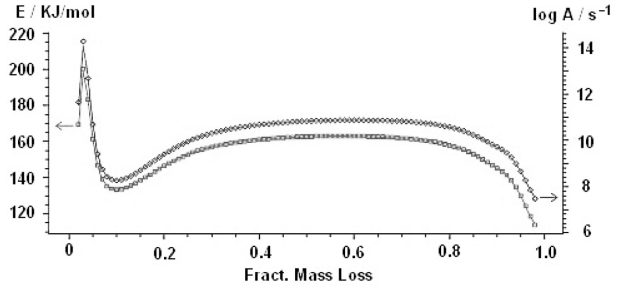

***Fig*. 3.** Apparent activation energy at various conversion degree of AP/Al (60/40) mixture calculated by model-free Friedman analysis.

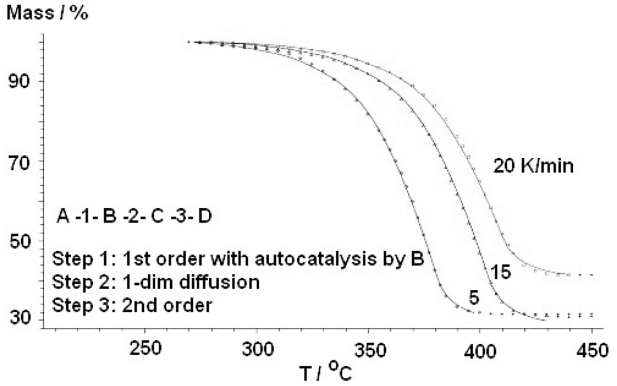

***Fig*. 4.** Global model for the decomposition of AP/Al (60/40) mixture.

(A, B, C and D stand for reagents, "→" stands for one step.) was taken into account to describe this process. Some statistical criteria, especially correlation coefficient, were applied to decide the best fit, which is shown in *Fig*. 4. The corresponding kinetic parameters are tabulated in *Table* 1. The correlation coefficient here was 0.9998. The proposed model is as following:

The first step is 1st order autocatalysis by B (C1B): $f(\alpha) = (1-\alpha)(1+K_{at}\alpha)$ (K_{at} is the autocatalytic order). The activation energy is 168 kJ/mol with log A of 13.01 s^{-1} and logK_{at} 1 of −3.

The second is one-dimension diffusion reaction (D1): $f(\alpha) = 1/\alpha^{-1}$. The activation energy is 163 kJ/mol with log A of 10.62 s^{-1}.

The third is 2nd order reaction (F2): $f(\alpha) = (1-\alpha)^2$, and the activation energy is 153 kJ/mol with log$A$ of 10.8 s^{-1}.

The model for thermal decomposition process of AP was obtained by the same way and it was demonstrated to be C1B→D1→D1. The third step was different to that of AP/Al. The decomposition mechanism of AP was changed after addition of nano-sized Al. Compared to the kinetic parameters of AP, shown in *Table* 1, the decrease in the activation energy of the third step for the AP/Al mixture

***Table* 1.** Kinetic parameters of thermal decomposition of AP and AP/Al (60/40) calculated by multivariate non-linear regression

	A→B			B→C		C→D	
	log *A* (s^{-1})	*E* (kJ/mol)	log *Kat*1	log *A* (s^{-1})	*E* (kJ/mol)	log *A* (s^{-1})	*E* (kJ/mol)
AP/Al	13.01	168	−3	10.62	163	10.80	153
AP	1.58	52	0.79	8.31	142	14.28	218

indicates the catalysis effects of Al nanoparticles on HTD of AP. The obstructed effects of Al nanoparticles on LTD of AP were supported by an increase in the activation energy of the first step.

MS/FTIR Analysis

In order to check and evaluate the proposed mechanisms described above, the non-isothermal thermal decomposition process was monitored by MS and FTIR on-line with a heating rate of 10 K/min.

The mass spectra results of gas products from AP and the AP/Al (60/40) mixture, tabulated in *Table* 2, shows the m/z 14, 15, 16, 17, 18, 28, 30, 31, 32, 35, 44 and 46 were detected. The possible assignments for the main ion numbers and the peak, onset and end temperatures are also summarized in *Table* 2. It is difficult to determine the onset and end temperatures for m/z 15, 16, 31, 35 and 44 since there was a lot of noise.

Fig. 5 represents FTIR spectra of gas products produced from AP and the AP/Al mixture at the time when the intensity of FTIR series is the maximum. Combined with the data in *Fig.* 5 and *Table* 2, it is certain that there are N_2O (2238 cm^{-1} and 2201 cm^{-1}), NO_2 (1630 cm^{-1} and 1598 cm^{-1}), H_2O (3500–4000 cm^{-1}), NO (1908 cm^{-1}), HCl (2700–3012 cm^{-1}), HNO_3 (1710 cm^{-1}) and $HClO_4$ (1120 cm^{-1}) for both compositions. The main gas products

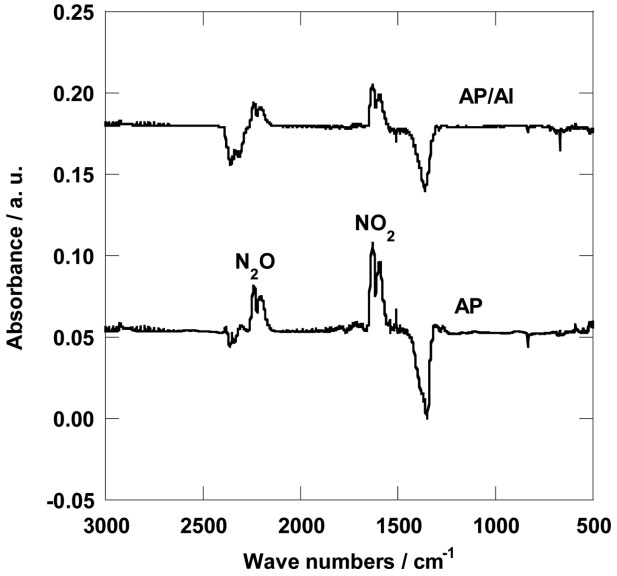

***Fig.* 5.** FTIR spectra of gas products of AP and AP/Al (60/40) mixture at a given time.

are N_2O and NO_2 based on the absorbance intensity. Their strongest absorbance intensities (2238 cm^{-1} for N_2O and 1630 cm^{-1} for NO_2) versus temperatures are depicted in *Fig.* 6. It shows that this process for both compositions can be divided into three steps, which is consistent with the results from TG-DSC. In case of neat AP, the first one is

***Table* 2.** Possible assignment, peak, onset and end temperatures of ions detected by MS

m/z	ion	T_p / °C		$T_o - T_e$ / °C	
		AP	AP/Al	AP	AP/Al
14	N^+	426	400	–	–
15	NH^+	436	399	–	–
16	NH_2^+, O^+	434	395	–	–
17	NH_3^+, OH^+	436	401	270–460	330–460
18	NH_4^+, H_2O^+	436	403	270–460	300–470
28	N_2^+	–	401	–	330–420
30	NO^+	432	399	270–350; 350–470	290–430
31	HNO^+	432	397	–	–
32	H_2NO^+, O_2^+, $N_2H_4^+$	430	399	270-450	290–440
35	Cl^+	434	410	–	–
44	N_2O^+	430	399	270–360; 350–480	300–430
46	NO_2^+	434	410	–	–

T_p–Peak temperature, °C; T_o–Onset temperature, °C; T_e–End temperature, °C.

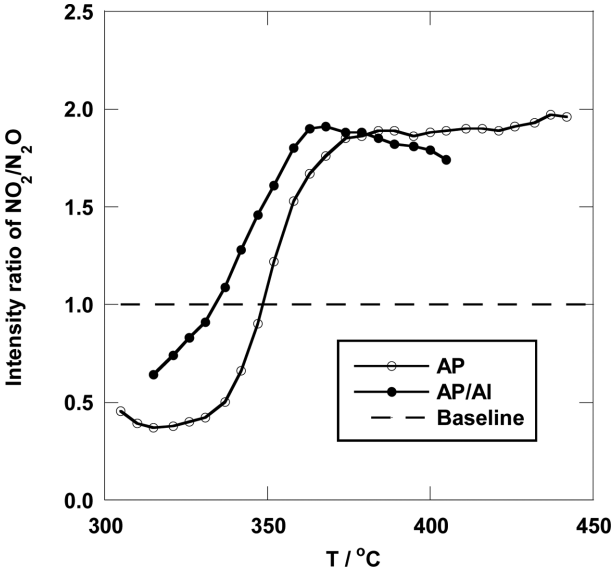

***Fig.* 6.** Dependences of FTIR intensity ratio of NO_2 to N_2O produced of AP and AP/Al (60/40) mixture on temperature.

from 280 °C to 350 °C, where the absorbance intensity of N_2O was greater than NO_2, suggesting the reaction of N_2O dominates the thermal decomposition although the ratio of NO_2 to N_2O is increasing in this stage. The second step is from 350 °C to 380 °C, where the ratio of NO_2 to N_2O continues to increase and the absorbance intensity of NO_2 was over N_2O, suggesting the reaction of NO_2 dominates the thermal decomposition. The third one is from 380 °C to 450 °C, where the ratio of NO_2 to N_2O is almost constant, indicating the thermal decomposition process is in a stable stage. The similar results were obtained for the AP/Al (60/40) mixture, as shown in *Fig.* 6. However, the onset and end temperatures for each step are different to AP. They are from 300 °C to 333 °C, 333 °C to 365 °C and 365 °C to 410 °C, respectively. Compared to AP, the onset temperature of the first step was increased and the third step decreased, suggesting that addition of 40 nm Al hinders LTD of AP and catalyzes HTD.

Isothermal Analysis

The isothermal method was used to predict the thermal stability of AP and the AP/Al (60/40) mixture based on the global kinetic model of thermal decomposition proposed above. The isothermal simulations with the temperatures from 130 °C to 200 °C were performed with a total exposition time of 10 hours. The results are shown in *Fig.* 7. The mass loss of thermal decomposition of AP at 150 °C reached 8%, while it was almost not changed for the AP/Al mixture at the same condition. It indicates that

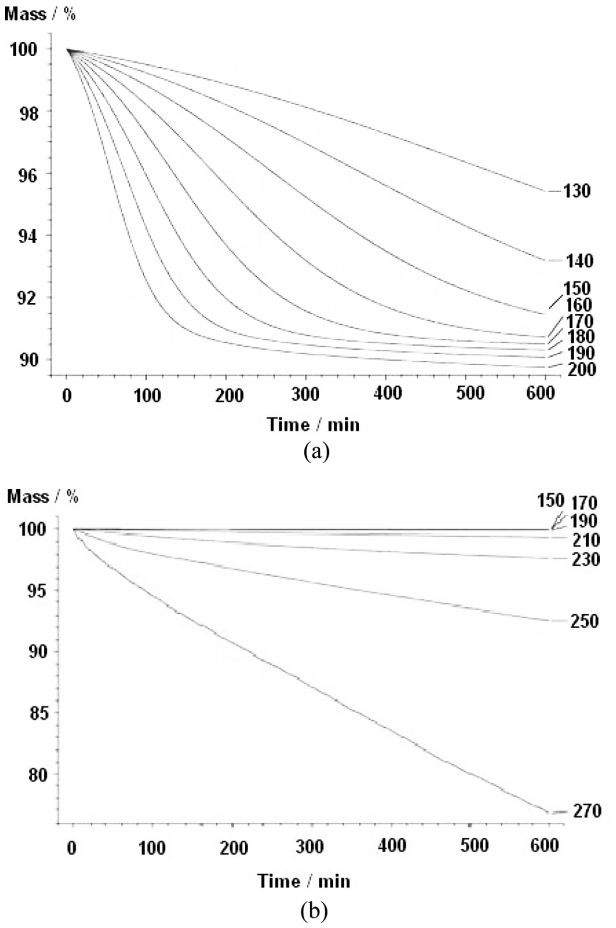

***Fig.* 7.** Simulated total mass loss under isothermal conditions for (a) AP and (b) AP/Al (60/40) mixture.

the thermal stability of AP is improved after addition of nano-sized Al at low temperatures and Al nanoparticls hinder LTD of AP.

CONCLUSIONS

The low-temperature thermal decomposition of AP was hindered and the high-temperature decomposition was catalyzed after addition of Al nanoparticles into AP probably due to the huge specific surface area of nano-sized Al. Three-step kinetic model of C1/D1/F2 for the AP/Al (60/40) mixture was proposed based on the dependence of activation energy of E, calculated by Friedman method, on the conversion degree of α, while it was C1/D1/D1 for neat AP. The thermal stability of AP at low temperatures was improved in the presence of nano-sized Al mostly caused by the absorption and constrained effects of Al on AP.

REFERENCES

1. Rajić, M.; Sućeska, M. Study of Thermal Decomposition Kinetics of Low-temperature Reaction of Ammonium Perchlorate by Isothermal TG. *J. Therm. Anal. Calorim*. **2001**, *63*, 375.
2. Raha, K.; Ramamurthy, S.; Patil, D. G. The Catalytic Effect of Rare Earth Oxides on the Thermal Decomposition of Ammonium Perchlorate. *J. Therm. Anal.* **1989**, *35*, 1205.
3. Ma, Z.; Li, F.; Chen, A. Preparation and Thermal Decomposition Behavior of TMOs/AP Composite Nanoparticles. *Nanoscience* **2006**, *11*, 142.
4. Fujimura, K.; Miyake, A. The Effect of Specific Surface Area of TiO_2 on the Thermal Decomposition of Ammonium Perchlorate. *J. Therm. Anal. Calorim*. **2010**, *99*, 27.
5. Wang, J.; He, S.; Li, Z.; Jing, X.; Zhang, M.; Jiang, Z. Synthesis of Chrysalis-like CuO Nanocrystals and Their Catalytic Activity in the Thermal Decomposition of Ammonium Perchlorate. *J. Chem. Sci.* **2009**, *121*, 1077.
6. Heng, B.; Xiao, T.; Hua, X.; Ming, Y.; Wei, T.; Wei, H.; Tang, Y. Catalytic Activity of Cu_2O Micro-particles with Different Morphologies in the Thermal Decomposition of Ammonium Perchlorate. *Thermochim. Acta* **2011**, *524*, 135.
7. Chen, L.-J.; Li, G.-S.; Li, L.-P. CuO Nanocrystals in Thermal Decomposition of Ammonium Perchlorate Stabilization, Structural Characterization and Catalytic Activities. *J. Therm. Anal. Calorim*. **2008**, *91*, 581.
8. Joshi, S. S.; Patil, P. R.; Krishnamurthy, V. N. Thermal DEcomposition Of Ammonium Perchlorate In The presence of Nanosized Ferric Oxide. *Defence Science Journal* **200**8, *58*, 721.
9. Survasea, D. V.; Sarwadea, D. B.; Kurian, E. M. Effect of La_2O_3, Pr_2O_3 and Nd_2O_3 on the Thermal Decomposition of Ammonium Perchlorate. *Journal of Energetic Materials* **2001**, *19*, 023.
10. Dedgaonkar, V. G.; Sarwade, D. B. Effects of Different Additives on the Thermal Decomposition of Ammonium Perchlorate. *J. Therm. Anal*. **1990**, *36*, 223.
11. Li, C.; Ma, Z.; Zhang, L.; Qian, R. Preparation of Ni/TiO_2 Nanoparticles and Their Catalytic Performance on the Thermal Decomposition of Ammonium Perchlorate. *Chin. J. Chem.* **2009**, *27*, 1863.
12. Song, M.; Chen, M.; Zhang, Z. Effect of Zn Powders on the Thermal Decomposition of Ammonium Perchlorate. *Propellants Explos. Pyrotech.* **2008**, *33*, 261.
13. Duan, H.; Lin, X.; Liu, G.; Xu, L.; Li, F. Synthesis of Co Nanoparticles and Their Catalytic Effect on the Decomposition of Ammonium Perchlorate. *Chin. J. Chem. Eng*. **2008**, *16*, 325.
14. Zhi, J.; Wang, T.; Li, S.; Zhao, F.; Liu, Z.; Yang, C.; Yang, L.; Liu, S.; Zhang, G. Thermal Behavior of Ammonium Perchlorate and Metal Powders of Different Grades. *J. Therm. Anal. Calorim*. **2006**, *85*, 315.
15. Liu, L.; Li, F.; Tan, L.; Ming, L.; Yi, Y. Effects of Nanometer Ni, Cu, Al and NiCu Powders on the Thermal Decomposition of Ammonium Perchlorate. *Propellants Explos. Pyrotech*. **2004**, *29*, 34.
16. Rajendran, A. G.; Kartha, C. B.; Babu, V. V. Influence of Specific Surface Area of Aluminium Powder on the Reactivity of Aluminium/ammonium Perchlorate Composition. *Propellants Explos. Pyrotech.* **1997**, *22*, 226.
17. Stephens, M.; Sammet, T.; Petersen, E.; Carro, R.; Wolf, S.; Smith, C. Performance of Ammonium-perchlorate-based Composite Propellant Containing Nanoscale Aluminum. *J. Propul. Power* **2010**, *26*, 461.
18. Srinivas, V.; Chakravarthy, S. R. Computer Model of Aluminum Agglomeration on Burning Surface of Composite Solid Propellant. *J. Propul. Power* **2007**, *23*, 728.
19. Liu, L.; Li, F.; Tan, L.; Ming, L.; Yi, Y. Effects of Metal and Composite Metal Nanopowders on the Thermal Decomposition of Ammonium Perchlorate (AP) and the Ammonium Perchlorate/Hydroxyterminated Polybutadiene (AP/HTPB) Composite Solid Propellant. *Chin. J. Chem. Eng.* **2004**, *12*, 595.
20. Opfermann, J. Kinetic Analysis Using Multivariate Nonlinear Regression, *J Therm. Anal. Calorim*. **2000**, *60*, 641.
21. Shen, S.; Wu, B. The Thermal Decomposition of Ammonium Perchlorate (AP) Containing a Burning-rate Modifier, *Thermochim. Acta* **1993**, *223*, 135.
22. Majdaa, D.; Korobovb, A.; Filekc, U.; Sulikowskic, B.; Midgleyd, P.; Nicold, D. A.; Klinowski, J. Low-temperature Thermal Decomposition of Crystalline Partly and Completely Deuterated Ammonium Perchlorate. *Chem. Phys. Lett.* **2011**, *504*(4-6), 185.
23. Jiang, Z.; Zhao, F. Study on Effects of Nanometer Metal Powder on Thermal Decomposition of HMX. *J. Propu. Tech.* **2002**, *23*, 58.
24. Trunov, M. A.; Umbrajkar, S. M.; Schoenitz, M.; Mang, J. T. Oxidation and Melting of Aluminum Nanopowders. *J. Phys. Chem. B* **2006**, *110*, 13094.